INTERNATIONAL ATOMIC ENERGY AGENCY
UNITED NATIONS EDUCATIONAL, SCIENTIFIC AND CULTURAL ORGANIZATION

INTERNATIONAL CENTRE FOR THEORETICAL PHYSICS
34100 TRIESTE (ITALY) - P.O.B. 586 - MIRAMARE - STRADA COSTIERA 11 - TELEPHONES: 224281/2/3/4/5/6
CABLE: CENTRATOM - TELEX 460392-1

SMR/110/A - 2

WORKING PARTY

ON

"PHYSICS OF CONDENSED MATTER AT PLANETARY PRESSURES"

(20 August - 7 September 1984)

POLYMORPHIC TRANSITIONS

I : Polymorphism of common minerals

A.B. THOMPSON

Dept. für Erdwissenschaften
E.T.H. Zürich, CH-8092
Switzerland

NATURALLY ABUNDANT OXIDES AND ROCK-FORMING MINERALS

SiO_2												
TiO_2	Fe_2TiO_4	$FeTiO_3$ $CaTiO_3$										
Al_2O_3	$MgAl_2O_4$	Al_2O_3										Al_2SiO_5
Fe_2O_3	Fe_3O_4	Fe_2O_3										
FeO	Fe_2SiO_4	$FeSiO_3$			$Fe_3Al_2Si_3O_{12}$							
MgO	Mg_2SiO_4	$MgSiO_3$			$Mg_3Al_2Si_3O_{12}$							
CaO	$CaMgSiO_4$ $CaAl_2O_4$	$CaMgSi_2O_6$ $CaAl_2SiO_6$	$CaAl_2Si_2O_8$		$Ca_3Al_2Si_3O_{12}$						$CaCO_3$	$CaCO_3$
Na_2O	$NaAlSiO_4$	$NaAlSi_2O_6$	$NaAlSi_3O_8$									
K_2O	$KAlSiO_4$	$KAlSi_2O_6$	$KAlSi_3O_8$	$KMg_3AlSi_3O_{10}(OH)_2$								
H_2O	$Mg(OH)_2$	$NaAlSi_2O_6.H_2O$										
CO_2												
C												
Fe	FeS											
S	FeS_2											
VECTORS	SiH_{-4}, $MgFe^{II}_{-1}$, $CaMg_{-1}$, NaK_{-1}, $AlFe^{III}_{-1}$, $Al_2Mg_{-1}Si_{-1}$, $CaAlNa_{-1}Si_{-1}$, $NaAl\square_{-1}Si_{-1}$, $Fe^{III}_2Fe^{II}_{-1}Ti_{-1}$											

Diamond
C

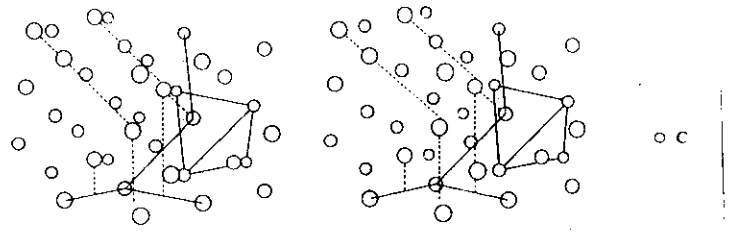

FIGURE II.64 Crystal structure of diamond.

Zoltai & Stout (1984)

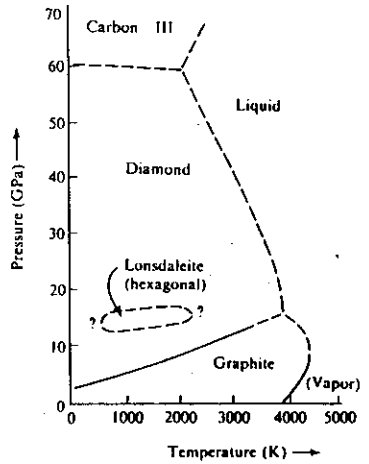

FIGURE II.65 Pressure-temperature phase diagram for the carbon system.

Graphite (*2H*)

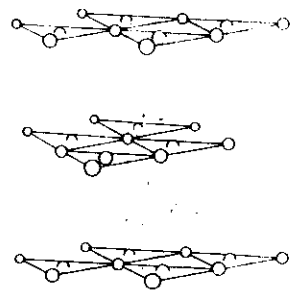

FIGURE II.66 Crystal structure of graphite, *c* axis vertical.

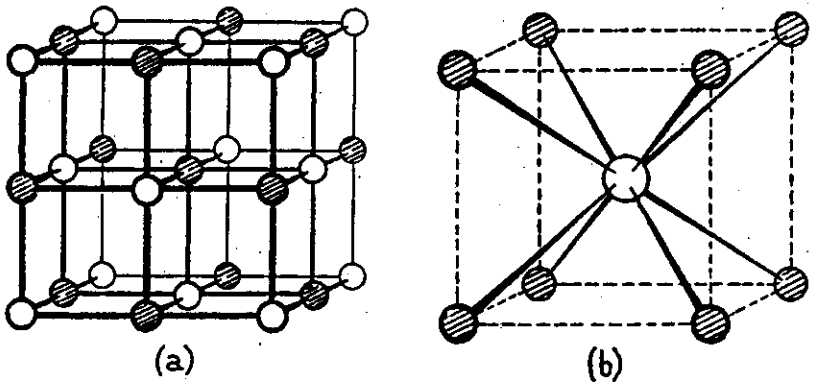

FIG. 17. The sodium chloride (NaCl) and caesium chloride (CsCl) structures.

Hazen & Finger (1982)

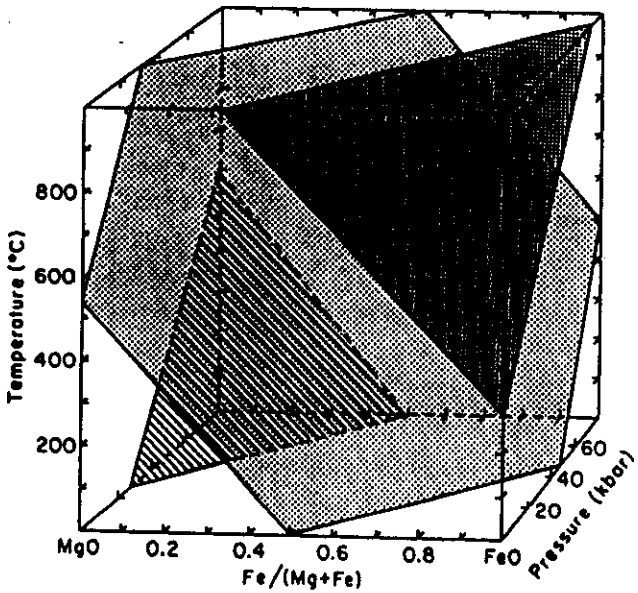

Figure 9-1. Isostructural surfaces for (Mg, Fe)O in *T–P–X* space

Wells (1962)

TABLE 83. *The crystal structures of some metallic oxides*

Type of structure	*Coordination numbers of* M *and* O *and formula type*	*Name of structure*	*Examples*
Infinite 3-dimensional complexes	6:2 MO_3	ReO_3	WO_3*
	8:4 MO_2	Fluorite	ThO_2, CeO_2, HfO_2, NpO_2, PuO_2, AmO_2, PoO_2, CmO_2, PrO_2,[a] UO_2,[b] ZrO_2[c]
	6:3 MO_2	Rutile	TiO_2, GeO_2, SnO_2, MnO_2, RuO_2, OsO_2, IrO_2, CrO_2, MoO_2,[d] WO_2*, TcO_2*, ReO_2,*[d] PbO_2,[d] VO_2,* (NbO_2),[e] TeO_2[f]
	6:4 M_2O_3	Corundum	α-Al_2O_3, α-Fe_2O_3, Cr_2O_3, Ti_2O_3, V_2O_3, α-Ga_2O_3, Rh_2O_3
	$x:x$‡ M_2O_3	'A' rare-earth sesquioxide	La_2O_3, Ce_2O_3, Pr_2O_3, Nd_2O_3
	6:4 M_2O_3	'C' rare-earth sesquioxide	α-Mn_2O_3, Sc_2O_3, Y_2O_3, In_2O_3, Tl_2O_3, Sm_2O_3, and other rare-earth oxides M_2O_3
	6:6 MO	Sodium chloride	MgO, CaO, SrO, BaO, CdO VO,† TiO,† NbO,† FeO,*[g] CoO,*[g] NiO,*[g] MnO*[g]
	4:4 MO	Zinc-blende / Wurtzite	BeO / ZnO
	4:2 MO_2	Silica structures	SiO_2, GeO_2
	2:4 M_2O	Cuprite	Cu_2O, Ag_2O
	4:8 M_2O	Anti-fluorite	Li_2O, Na_2O, K_2O, Rb_2O
Layer structures	..	..	MoO_3, As_2O_3, PbO
Chain structures	..	..	Sb_2O_3, CrO_3 SeO_2
Molecular: structural units: polymers			Sb_4O_6, As_4O_6
,, ,, single molecules			All simple molecular oxides

* Distorted variant of the structure. † Defect structure. ‡ See text (p. 464).

[a] Below 350° C and under oxygen pressure of less than 10 atm there are two phases, Pr_6O_{11} and PrO_2 (C. L. Sieglaff and L. Eyring, *JACS*, 1957, 79, 3024).

[b] See also p. 965.

[c] Fluorite structure at high temperatures, monoclinic structure at ordinary temperature in which Zr^{4+} is 7-coordinated (J. D. McCullough and K. N. Trueblood, *Acta Cryst.*, 1959, 12, 507). HfO_2 also crystallizes with this structure (J. Adam and M. D. Rogers, ibid., p. 951).

[d] Also α-PbO_2 (columbite) structure.

[e] Superstructure of rutile with 32 NbO_2 in unit cell (A. Magnéli *et al.*, *Acta Chem. Scand.*, 1955, 9, 1402).

[f] A brookite-like form (T. Ito and H. Sawada, *Z. Krist.*, 1939, 102, 13) and a third (tetragonal) form (B. Stehlik and L. Balák, *Coll. Czech. Chem. Comm.*, 1949, 14, 595) have also been described.

[g] Less symmetrical variants of the NaCl structure at lower temperatures: FeO, NiO, and MnO (rhombohedral) and CoO (tetragonal). For references see J. S. Smart and S.

TABLE II.1. *Silica Minerals and Their Structural Derivatives*

Silica Mineral	Tetrahedral Substitution per one Si in SiO_2	Extra Cation per Tetrahedral Substitution	Derivative Silicate	
Coesite	$\frac{1}{4}Al^{3+}$	$\frac{1}{4}K^{1+}$	Microcline	KSi_3AlO_8
Coesite	$\frac{1}{4}Al^{3+}$	$\frac{1}{4}Na^{1+}$	Albite	$NaSi_3AlO_8$
Coesite	$\frac{1}{4}Al^{3+}$	$\frac{1}{4}Ca^{2+}$	Anorthite	$CaSi_2Al_2O_8$
Tridymite	$\frac{1}{4}Al^{3+}$	$\frac{1}{4}K^{1+}$	Kalsilite	$KSiAlO_4$
Tridymite	$\frac{1}{4}Al^{3+}$	$\frac{1}{4}Na^{1+} + \frac{1}{4}K^{1+}$	Nepheline	$KNa_3Si_4Al_4O_{16}$
Cristobalite	$\frac{1}{4}Al^{1+}$	$\frac{1}{4}Na^{1+}$	Carnegieite	$NaSiAlO_4$
High quartz	$\frac{1}{4}Al^{3+}$	$\frac{1}{4}Li^{1+}$	Eucryptite	$LiSiAlO_4$
Keatite*	$\frac{1}{4}Al^{3+}$	$\frac{1}{4}Li^{1+}$	High spodumene	$LiSi_2AlO_6$

* Does not occur naturally.

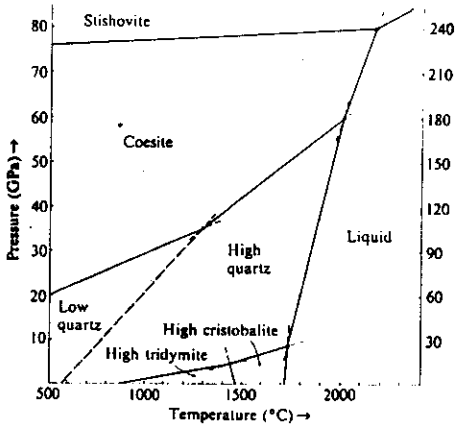

FIGURE II.1 Pressure-temperature phase diagram for SiO_2 polymorphs. Long dashes represent possible second-order transition. Short dashes represent metastable extensions of univariant reaction curves.

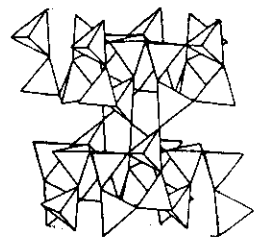

FIGURE II.5 Crystal structure of coesite, *b* axis vertical.

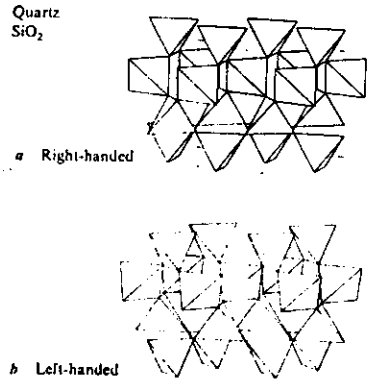

FIGURE II.2 Crystal structure of high quartz, *c* axis vertical. (a) right-handed, (b) left-handed.

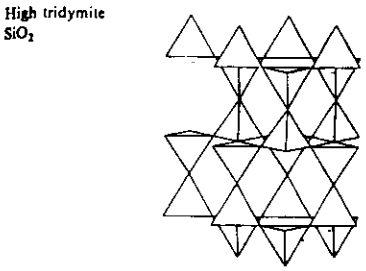

FIGURE II.3 Crystal structure of high tridymite, *c* axis vertical.

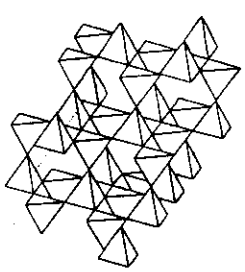

FIGURE II.4 Crystal structure of high cristobalite, [111] direction vertical.

Zoltai & Stout (1984)

1.4

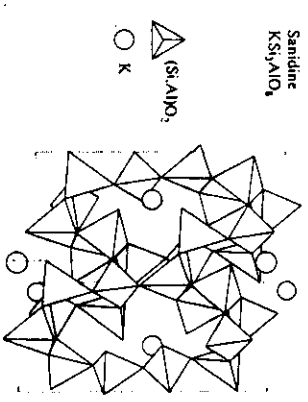

FIGURE II.8 Crystal structure of sanidine, *b* axis vertical.

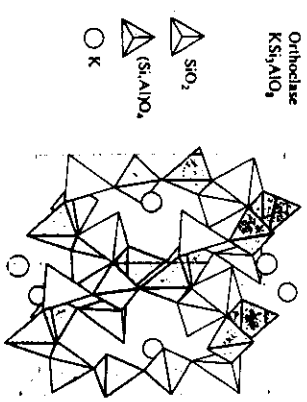

FIGURE II.9 Crystal structure of orthoclase, *b* axis vertical.

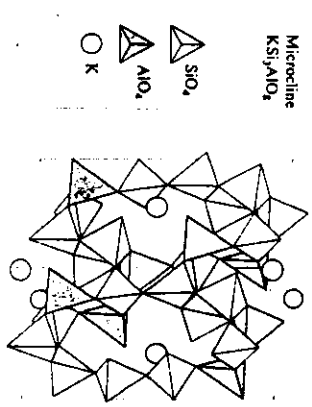

FIGURE II.10 Crystal structure of maximum microcline, *b* axis vertical.

Zoltai & Stout (1984)

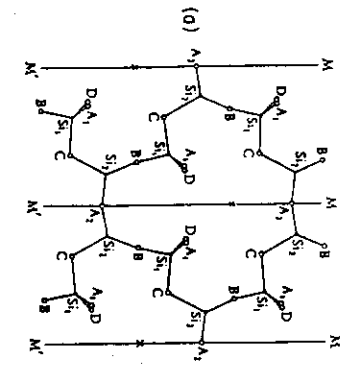

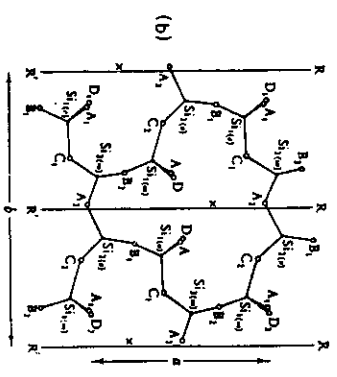

Figure 10-2. Monoclinic (a) and triclinic (b) modifications of the alkali feldspars $(K,Na)AlSi_3O_8$. (From Deer *et al.*, 1963, reproduced by permission of Longman's Group)

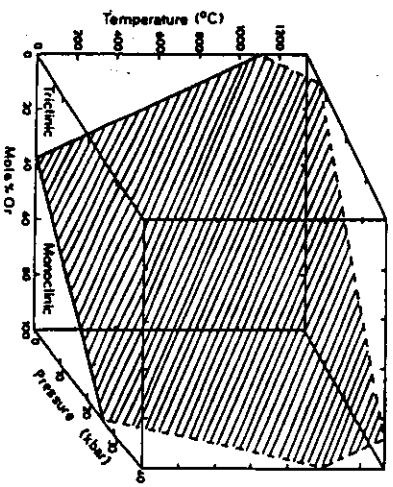

Figure 10-3. Polyhedral tilt transition surface in *T–P–X* space for the monoclinic-to-triclinic transition in alkali feldspars. (From Hazen, 1976, *Science* 194, 105–107. Copyright 1976 by the American Association for the Advancement of Science)

Hazen & Finger (1982)

1.5

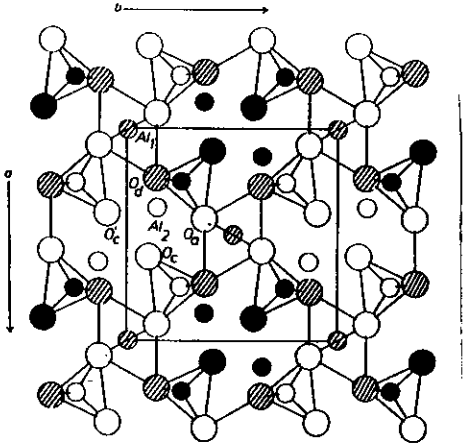

Fig. 1. Crystal structure of andalusite as projected parallel the *c*-axis. *Shaded circles* represent atoms at Z=0, *striped circles* represent atoms at Z≈1/4 and *clear circles* represent atoms at Z=1/2. The lattice constants are: a=7.794 Å, b=7.898 Å, c=5.559 Å

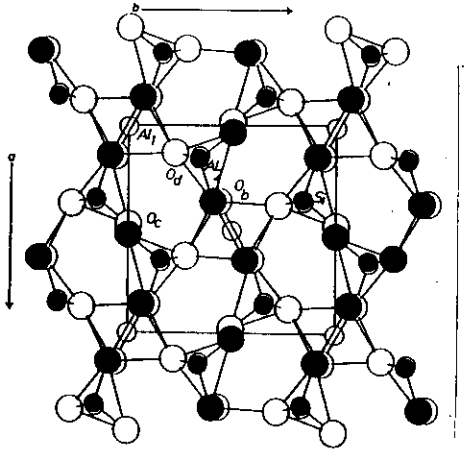

Fig. 2. Crystal structure of sillimanite. The axes are denoted according to the space group Pbnm. The upper atoms are shaded. The lattice constants are: a=7.485 Å, b=7.674 Å, c=5.770 Å

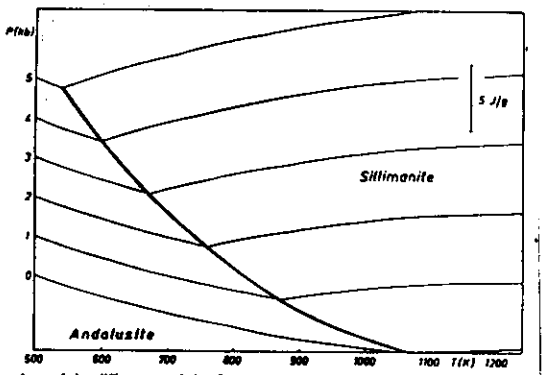

Fig. 10. Absolute values of the differences of the Gibbs free energies of sillimanite and andalusite $|G_{sillimanite} - G_{andalusite}|$. The y-axis is $|\Delta G|$ for each curve, the unit of 5 J/g is denoted by the bar at the upper right hand side of the diagram. The different curves are isobars, their origin is shifted for each isobar for the sake of clarity. The corresponding pressure is indicated at the ordinate. The minima ($\Delta G = 0$) represent the equilibrium conditions and are connected by the thick line which indicates the phase boundary.

Salje & Wernecke (1982)

Zoltai & Stout (1984)

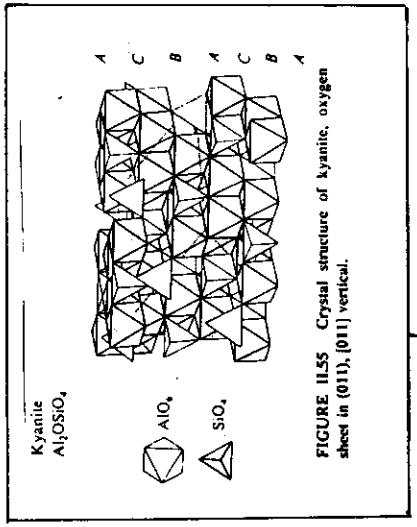

FIGURE 11.55 Crystal structure of kyanite, oxygen sheet in (011), [011] vertical.

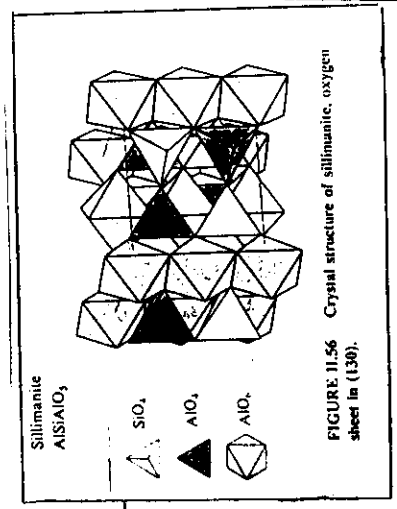

FIGURE 11.56 Crystal structure of sillimanite, oxygen sheet in (130).

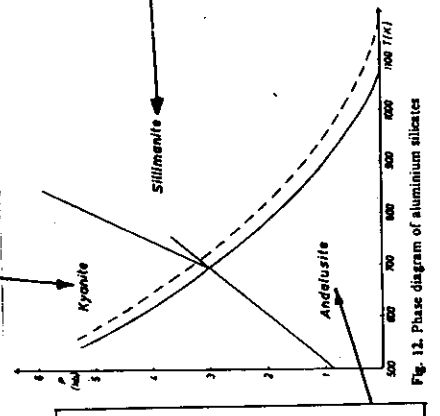

Fig. 12. Phase diagram of aluminium silicates

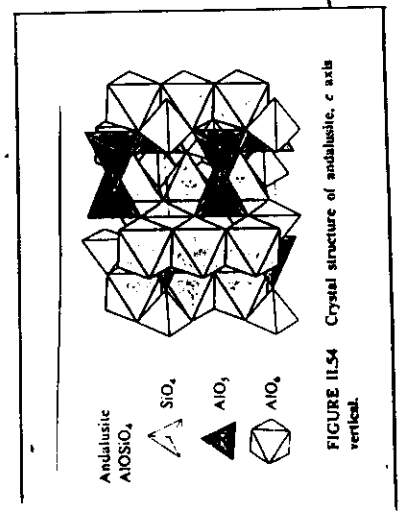

FIGURE 11.54 Crystal structure of andalusite, *c* axis vertical.

Zoltai & Stout (1984)

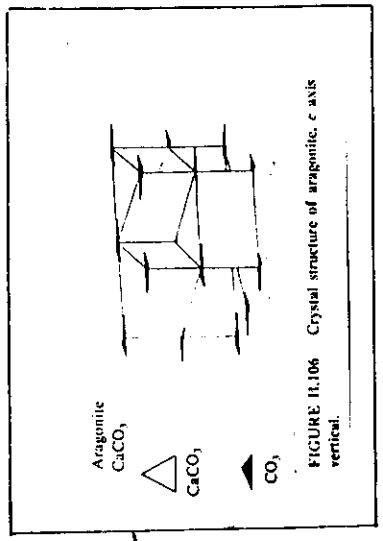

FIGURE 11.106 Crystal structure of aragonite, c axis vertical.

Mirwald (1976)

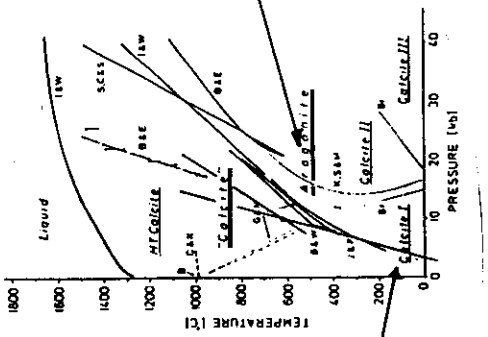

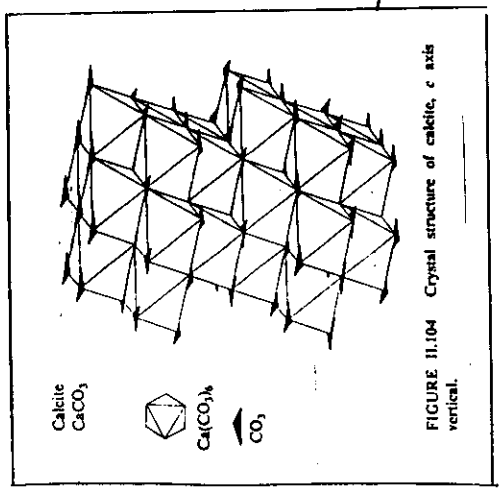

FIGURE 11.104 Crystal structure of calcite, c axis vertical.

REFERENCES

Hazen, R.M. (1977) : Effects of temperature and pressure on the crystal structure of ferromagnesian olivine. Amer. Mineral. 62, 286-295.

Hazen, R.M. & Finger, L.W. (1982) : Comparative Crystal Chemistry. John Wiley & Sons, New York, 231 p.p.

Ito, E. & Matsui, Y. (1977) : Silicate Ilmenites and post-spinel transformations pp. 193-208 in High-Pressure Research: Applications to Geophysics, eds. Manghnani, M.H. & Akimoto, S; Academic Press, New York, 642 pp.

Jamieson, J.C. (1977) :Phase transitions in Rutile type structures, p.p. 209-218. in High-Pressure Research: Applications to Geophysics, eds. Manghnani, M.H. & Akimoto, S; Academic Press, New York, 642 pp.

Mirwald, P. (1976) : A differential thermal analysis study of the high temperature polymorphism of calcite at high pressure. Contrib. Mineral. Petrol. 59, 33-40.

Ringwood, A.E. (1975) : Composition and Petrology of the Earth's Mantle. McGraw-Hill, New York, 618 pp.

Salje, E. & Wernecke, Ch. (1982) : How to determine phase stabilities from lattice vibrations. pp. 321-348, in High-Pressure researches in Geoscience, ed. Schreyer, W.E., Schweizerbart'sche Verlagsbuchhandlung, Stuttgart.

Suito, M. (1977) : Phase relations of pure Mg_2SiO_4 up to 200 kbars. pp. 255-266, in High-Pressure Research: Applications to Geophysics, eds. Manghnani, M.H. & Akimoto, S; Academic Press, New York, 642 pp.

Sung, C.M. & Burns, R.G. (1978) : Crystal structural features of the olivine - spinel transition. Phys. Chem. Minerals, 2, pp. 177-197.

Wells, A.F. (1962) : Structural Inorganic Chemistry. Clarendon Press, Oxford 1055 pp.

Zoltai, T. & Stout, J.H. (1984) : Mineralogy:Concepts and principles. Burgess Pub.Co., Minneapolis, 505 pp.